J. Inst. Electrostat. Jpn. 静電気学会誌，**34**, 2 (2010) 99−104

Paper

Emission Spectroscopy of Microplasma Driven by a Pulsed Power Supply*

Marius BLAJAN,**,[1] Shuichi MURAMATSU,** Tatsuya ISHII,**
Hidenori MIMURA*** and Kazuo SHIMIZU**

(Received August 3, 2009; Accepted March 22, 2010)

Emission spectrum of the microplasma discharge in N_2 or air with water droplets was analyzed. Two experimental Marx Generators were used as pulsed power supplies, with negative and positive pulse respectively. Emission spectra for N_2 gas with water droplets show N_2 second positive band system (N_2 SPS), N_2 first negative band system (N_2 FNS), H-γ band system, and OH peaks. For air with water droplets emission spectrum shows N_2 SPS, N_2 FNS and H-γ band system with lower intensities comparing with microplasma discharge in N_2 gas with water droplets. Emission signal of the photomultiplier, show short lifetime emission signal for N_2 SPS of 337.1 nm. Vibrational temperature calculation was also carried out using the N_2 second positive system ($C^3\Pi$ - $B^3\Pi$ band).

1. Introduction

Microplasma can be found in many applications. In the last years, the technology was used in applications such as NOx removal, surface treatment and sterilization or inactivation of bacteria. Although there is an interest for application driven research, microplasma phenomena are not fully understood. Emission spectroscopy is one of the methods to analyze plasma process.[1,2)]

The high intensity electric field generated between microplasma electrodes, charged particles, reactive ground state species, excited species, UV photons can affect the bacteria. Atmospheric microplasmas have been shown to inactivate a wide spectrum of microorganism including spores, Gram-negative bacteria, Gram positive bacteria and viruses.[3)] Research works showed that better results of bacteria inactivation using non thermal plasma were obtained with H_2O addition in comparison with dry processes.[4)] One of the processes of bacteria inactivation using microplasma consists in spraying water droplets containing bacteria through microplasma electrodes. Air or nitrogen is used as carrier gas.[5)] The high intensity electric field generated between microplasma electrodes, charged particles, reactive ground state species, excited species, UV photons can affect the bacteria. The analysis of these factors could be done by emission spectroscopy method. The aim of this paper is to analyze the emission spectrum of the microplasma in air and nitrogen containing water droplets.

2. Experimental Setup

2.1 Experimental Setup

The experimental setup is shown in Fig. 1. Emission spectra were measured by an ICCD camera (Ryoushi-giken, SMCP–ICCD 1024 HAM-NDS/UV), a spectrometer (Ryoushi-giken, VIS 351) and by a photomultiplier tube (Hamamatsu Photonics, R3896). A pulse generator (Tektronix, AFG 3021B) was used to trigger the Marx Generator consisted of semiconductor switches and the ICCD camera. Obtained data were transferred to a computer.

The discharge voltage and the corresponding discharge current were measured by a high voltage probe (Tektronix, P6015), an AC current transformer (Tektronix, P6021) and a digital oscilloscope (Tektronix, TDS 2014B).

The resolution of the ICCD measurements was carried out with FWHM 3ch. 3ch was set to 0.087 nm at narrow gratings carried out with 2,400 grooves. Spectrometer has three mirrors which are reflecting the light with a calculated reflectance of 90%. The measured intensity was 26% at 225 nm, 25% at 250

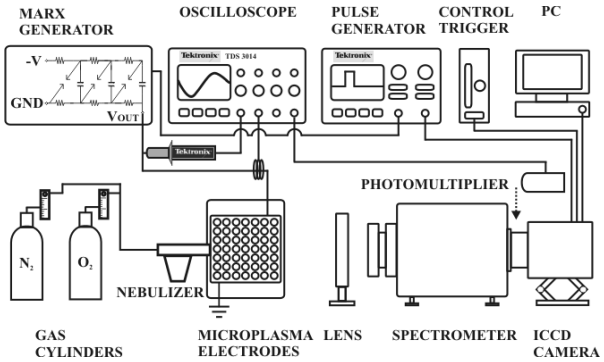

Fig. 1 An experimental setup.

Key Words：microplasma, pulsed power, emission spectroscopy.

* Marius BLAJAN, 村松秀一, 石井達也, 三村秀典, 清水一男：パルス電源を用いた大気圧マイクロプラズマの発光分析

** Innovation and Joint Research Center, Shizuoka University, 3-5-1, Nakaku, Hamamatsu 432−8561, Japan.

*** Research Institute of Electronics, Shizuoka University, 3-5-1, Nakaku, Hamamatsu 432-8561, Japan

[1] blajanmarius@yahoo.com

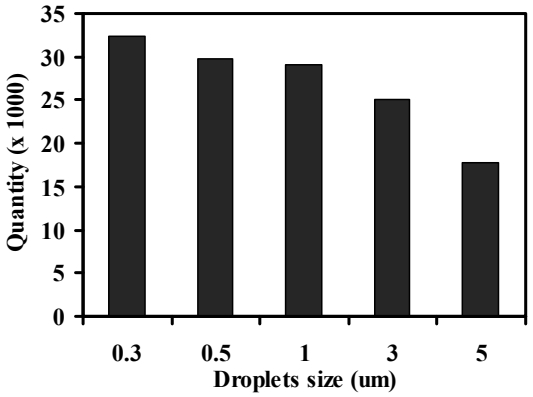

Fig. 2 The size distribution of water particles generated inside the nebulizer at a gas flow rate of 5 L/min.

nm and 23% at 275 nm respectively, with narrow gratings due to the reflectance of the mirrors and grating.

At wide grating settings with 200 grooves, the measured intensity was 53% at 360 nm, 63% at 400 nm and 68% at 440 nm, respectively.

Compositions of gases used in experiments were N_2, N_2 and water droplets, air and air with water droplets. Experiments were carried out in atmospheric pressure and the gas flow rate was set at 5 L/min. Water droplets were added in the carrier gas using a medical nebulizer. The water droplets sizes and distribution is presented in Fig. 2. The diameters of the water particles formed by the nebulizer were measured by a laser particle counter (Kanomax, 3886). With water added to the nebulizer, water droplets with diameters ranging from 0.5 μm to 5 μm were generated at the applied gas flow rate of 5 L/min.

The spectrometer settings can be set at wide gratings for a wide range of spectrum or narrow settings for measuring a specific range with greater accuracy.

ICCD camera functional elements sensitivities such as micro channel plate (MCP) and phosphor screen can be varied in order to measure the spectrum for different intensities.

2.2 Marx Generator

A Marx generator with 4 stages MOSFET switches shown in Fig. 3a, was developed to be used as high voltage negative polarity supply to microplasma electrodes. It has an output voltage up to −1.8 kV peak (negative pulse, rise time 80 ns, pulse width 500 ns −1 μs, frequency 1−24 kHz). Trigger signal for ICCD camera was set at 1 μs (Fig. 4).

Capacitors were charged in parallel connection at a given voltage V (500 V in this case). When the MOSFET switches were closed, capacitors were discharging in series connection thus results an output voltage $4V$ (2 kV in this case).

A Marx generator with 5 stages MOSFET switches for generating high voltage positive pulses was developed (Fig. 3b). An output voltage was up to 1.8 kV peak (positive pulse, rise time 80 ns, pulse width 1.5 μs, frequency 1−24 kHz).

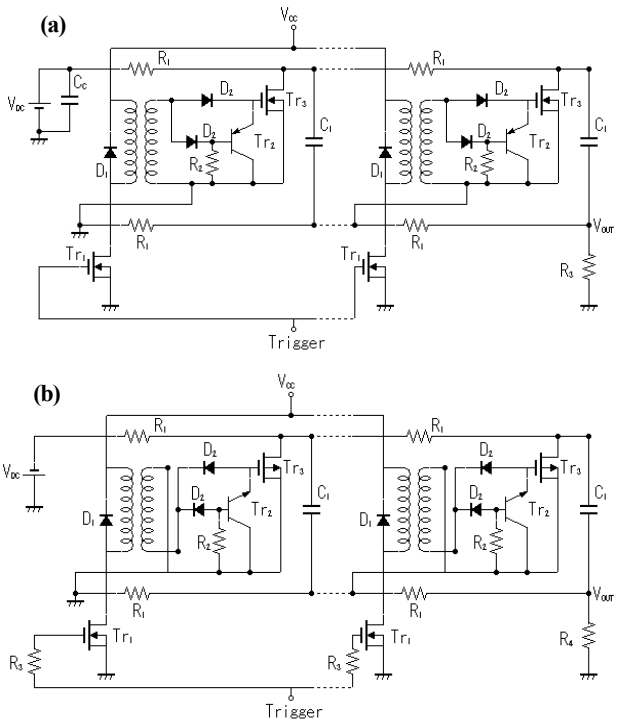

Fig. 3 An experimental Marx Generator: (a) with negative pulses; (b) with positive pulses.

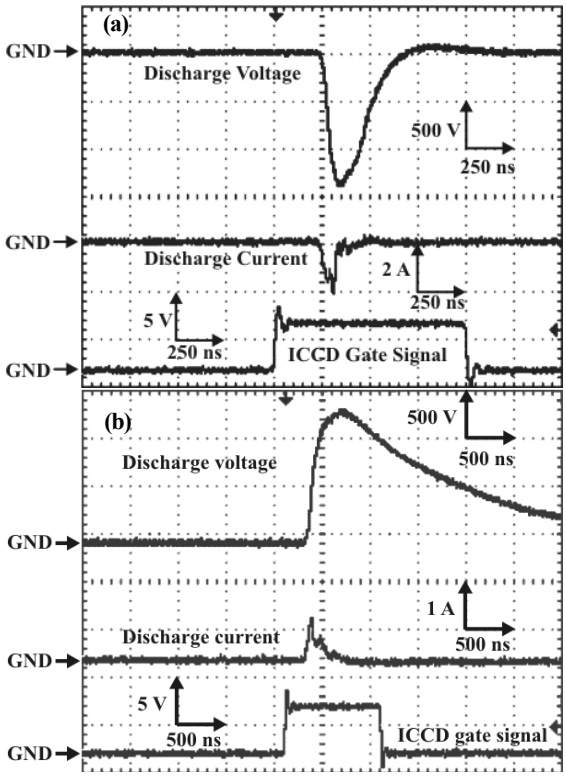

Fig. 4 Waveforms of discharge voltage, discharge current and gate signal for ICCD camera: (a) negative pulse; (b) positive pulse.

Trigger signal for ICCD camera was set at 1 μs (Fig. 4).

Figure 4 shows the typical waveforms of both negative (Fig. 4(a)) and positive (Fig. 4(b)) pulse circuit.

Discharge current was confirmed at rising point of discharge voltage. About -2 A was obtained at -1.4 kV for negative pulse.

Discharge current was also confirmed at rising point of discharge voltage for positive polarity. Discharge current was lower for the positive pulse (about 1 A at 1.4 kV). The MOSFET used in the positive pulse Marx Generator had longer rise time. Thus a difference occurred between discharge current peaks for negative pulse and positive pulse respectively at the same discharge voltage.

The use of pulsed power in various applications such as NOx removal or biomedical applications is advantageous because of the low cost of equipment and insignificant heating. Pulsed atmospheric plasma has a higher energy efficiency than the sinusoidal plasma due to the long time plasma off period that reduces power consumption.[6,7] In the microplasma processes such as NOx removal, is necessary less power to remove the same quantity of NO from exhaust gases by using a pulsed power supply in comparison with the case where AC voltage is used,[8,9] due to the reduced thermal load on electrodes at higher currents.[10]

3. About Microplasma

Microplasma electrodes used in this study were metallic electrodes covered with a dielectric layer (Fig. 5). Due to small discharge gaps (0−100) μm and to the assumed specific dielectric constant of $\varepsilon_r = 10^4$, a high intensity electric field (10^7−10^8 V/m) could be obtained with relatively low discharge voltages around 1 kV. Electrode size was 20 mm *versus* 40 mm..

Electrode has holes to flow for gas treatment, which diameter is Ø 2 mm and its aperture ratio of 36%. Discharge gap was set at 50 μm in this study.

Emission spectra of microplasma discharge was observed from the side part of electrodes. Thus the observed microplasma area had 40 mm *versus* 50 μm.

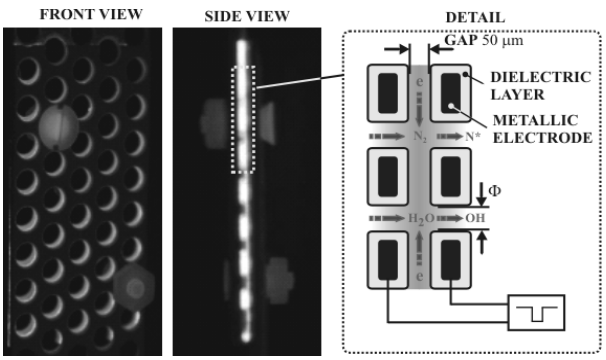

Fig. 5 Microplasma electrodes.

4. Emission Spectrum of Microplasma

4.1 Microplasma by negative pulses

Emission spectrum of the microplasma discharge in N_2 with water droplets showed peaks of N_2 second positive band system (N_2 SPS) and N_2 first negative band system (N_2 FNS) (Fig. 6).

This spectrum was obtained at discharge voltage −1.4 kV, rise time of 80 ns, pulse width of 500 ns, and discharge frequency of 1 kHz.

N_2 SPS (337.1, 357.7, 375.5, 380.5 nm) was observed due to the electron collision (Table 1). N_2 FNS peak was also observed at 427.8 nm as shown in Fig. 6.

Emission spectrum of the microplasma discharge in air with water droplets, showed peaks of N_2 SPS and N_2 FNS. Intensities of peaks were lower than those measured for nitrogen, due to the quenching effect of O_2.[11,12] These elementary processes described the radiation kinetics for the second positive band system of nitrogen, wavelength 337.1 nm, at atmospheric pressure:[13]

Excitation of nitrogen molecules in the ground state by direct electron impact:

$$e + N_2(X^1\Sigma_g^+)_{v=0} \rightarrow N_2(C^3\pi_u)_{v'=0} + e \quad (\Delta E=11eV) \quad (1)$$

Spontaneous radiation of formed excited state of nitrogen:

$$N_2(C^3\pi_u)_{v'=0} \rightarrow N_2(B^3\pi_g)_{v''=0} + h\nu \quad (\tau_o^C=40\ ns) \quad (2)$$

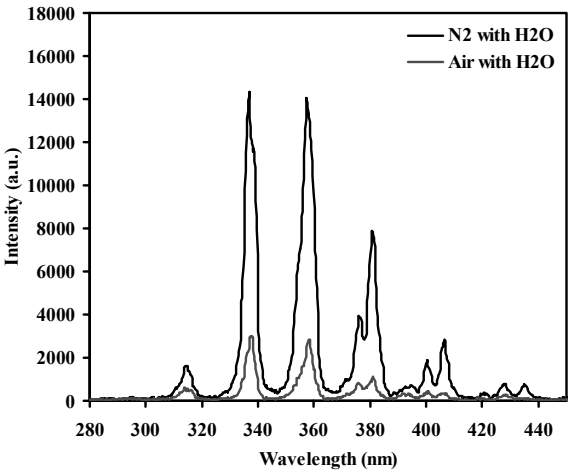

Fig. 6 Emission spectrum of microplasma discharge in N_2 with water droplets and air with water droplets for negative pulses.

Table 1 List of detected systems and peaks for the microplasma in N_2 gas and air with water droplets at wide gratings settings of the spectrometer.

Species (system)	Transition	Peak Position (nm)
N_2 second positive	$C^3\Pi \rightarrow B^3\Pi$	315; 337.1; 357.7; 375.5; 380.5; 400.0
N_2^+ first negative	$B^2\Sigma_u^+ \rightarrow X^2\Sigma_g^+$	427.8

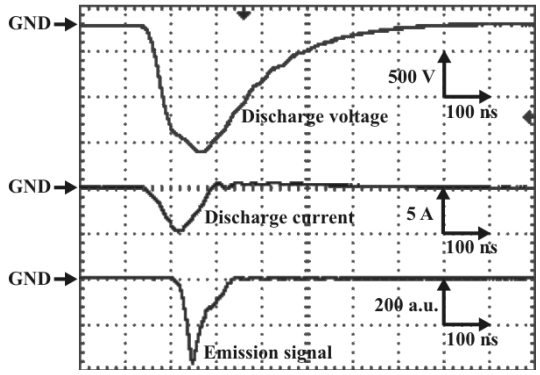

Fig. 7 Waveforms of discharge voltage, discharge current and emission signal of microplasma (N_2 SPS 337.1 nm) in N_2 with water droplets for negative pulses.

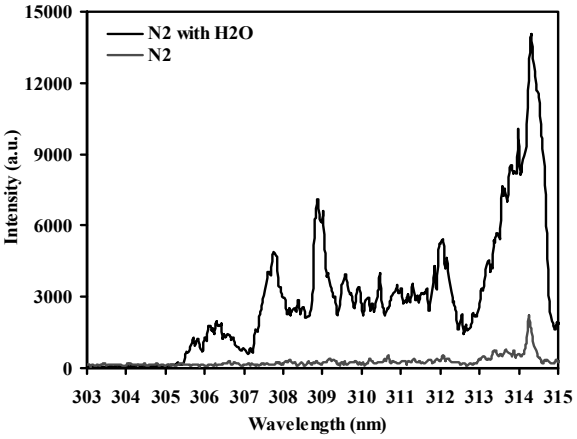

Fig. 8 Emission spectrum of microplasma generated by negative pulse in N_2 gas and in N_2 gas with water droplets for negative pulses.

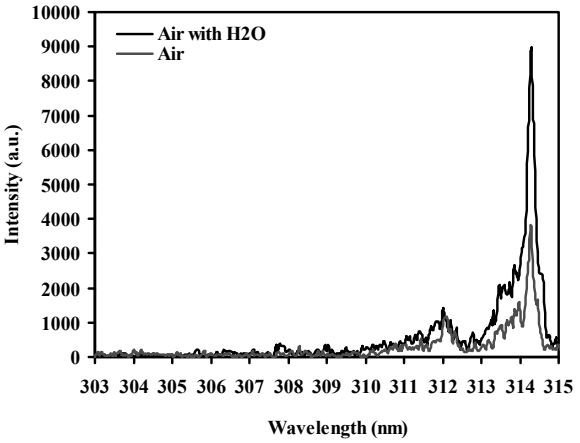

Fig. 9 Emission spectrum of microplasma discharge in air and in air with water droplets for negative pulses.

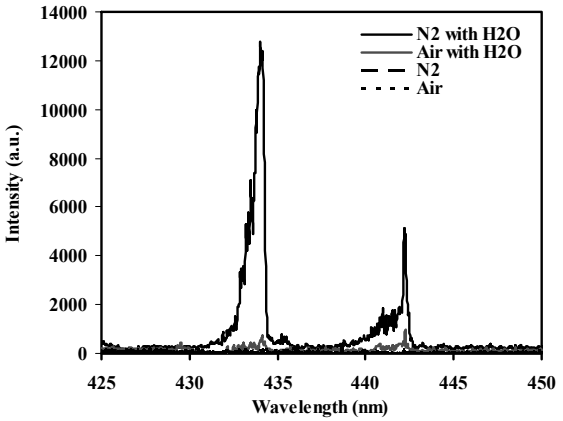

Fig. 10 Emission spectrum of microplasma discharge in N_2 or air with water droplets for negative pulses.

Figure 7 shows waveform of discharge voltage, discharge current and emission signal of photomultiplier corresponding to N_2 SPS wavelength of 337.1 nm..

The lifetime of photomultiplier signal of N_2 SPS was about 40 ns as shown in Fig. 7 and according with reaction (2).

The gratings of spectrometer were set at narrow settings in order to achieve a higher sensitivity of the MCP settings of ICCD camera on a distinct range of wavelengths.

In Fig. 8 is presented the emission spectrum of microplasma discharge in N_2 and in N_2 with water droplets. The spectrum for the N_2 gas containing water droplets showed the presence of the OH wavelengths at 306.4, 307.8 and 308.9 nm. An interference optical filter was used for measurements. The filter has the center wavelength at 309.5 nm with a peak transmission of 16.52%, and FWHM coordinates of 304.315 nm and 314.676 nm respectively.

Electron impact dissociation of H_2O leads to the production of H and OH radicals: [14]

$$e + H_2O \rightarrow e + H + OH \quad (3)$$

Air which used as carrier gas with water droplets, leads to the generation of active species and ozone by microplasma:[14,15]

$$e + O_2 \rightarrow e + O(^3P) + O(^1D) \quad (4)$$

$$O + O_2 + M \rightarrow O_3 + M \quad (5)$$

The excited state $O(^1D)$ O_2 dissociated H_2O to generate OH:[9]

$$O(^1D) + H_2O \rightarrow 2\,OH \quad (6)$$

The emission spectrum for air and air containing water droplets are presented in Fig. 9. With oxygen in the carrier gas, any peaks of OH were not observed due to the quenching effect of oxygen atom and ozone:[12,14]

$$OH + O \rightarrow O_2 + H \quad (7)$$

$$OH + O_3 \rightarrow HO_2 + O_2 \quad (8)$$

Emission spectrum of microplasma in N_2 or air with water droplets for 425 nm to 450 nm range is presented in Fig. 10. The peak of the hydrogen Balmer line H-γ is shown at 434.1 nm.[16,17] An interference optical filter was used for measurements. The filter has the center wavelength at 432.22 nm with a peak transmission of 55.32%, and FWHM coordinates of 432.747 and 441.7 nm respectively.

Hydrogen radicals react with oxidative species to generate OH or HO_2 radicals:

$$H + O^* \rightarrow OH^* \quad (9)$$

Table 2 List of detected systems and peaks for the microplasma in N_2 gas and air with water droplets at narrow gratings settings of the spectrometer.

Species (system)	Transition	Peak Position (nm)
N_2 second positive	$C^3\Pi \rightarrow B^3\Pi$	315; 337.1; 357.7; 375.5; 380.5; 400
N_2^+ first negative	$B^2\Sigma_u^+ \rightarrow X^2\Sigma_g^+$	427.8
OH (3064 – Å system)	$A^2\Sigma^+ \rightarrow X^2\Pi$	306.4; 307.8; 308.9[16, 17]
H-γ	$^2P^0 \rightarrow {}^2D$	434.1 [16, 17]

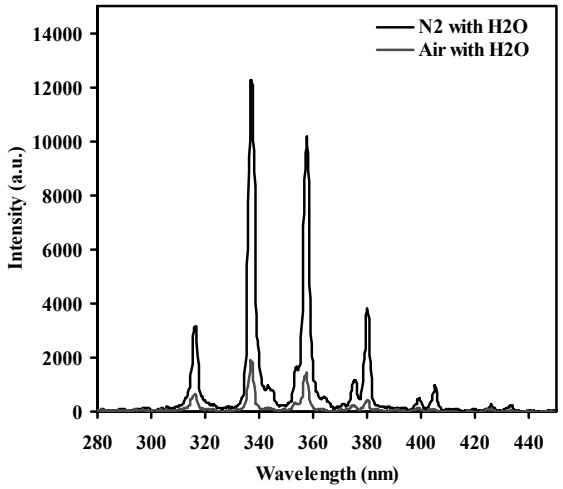

Fig. 11 Emission spectrum of microplasma discharge in N_2 gas and in N_2 gas with water droplets for positive pulses.

$$H + OH \rightarrow H_2O \quad (10)$$

$$H + O_2 \rightarrow HO_2^* \quad (11)$$

Thus the peaks of hydrogen could not be detected with oxygen.

The list of detected system and peaks for microplasma in N_2 gas and air with water droplets at narrow gratings settings of the spectrometer is showed in Table 2.

4.2 Microplasma by positive pulses

Emission spectrum of the microplasma discharge in N_2 with water droplets show peaks of N_2 second positive band system (N_2 SPS) and N_2 first negative band system (N_2 FNS) (Fig. 11).

This spectrum was obtained at discharge voltage 1.4 kV, rise time of 80 ns, pulse width of 1.5 μs, and discharge frequency of 1 kHz.

The emission spectrum is similar in shape with spectrum obtained at negative pulses.

The peaks of OH for the microplasma discharge at positive pulses in N_2 gas with water droplets are presented in Fig. 12. An interference optical filter was used to observe the weak signal.

The filter has the center wavelength at 309.5 nm with a peak transmission of 16.52%, and FWHM coordinates of 304.315 and 314.676 nm respectively. The results were similar to that of negative pulse. Production of H and OH radicals by

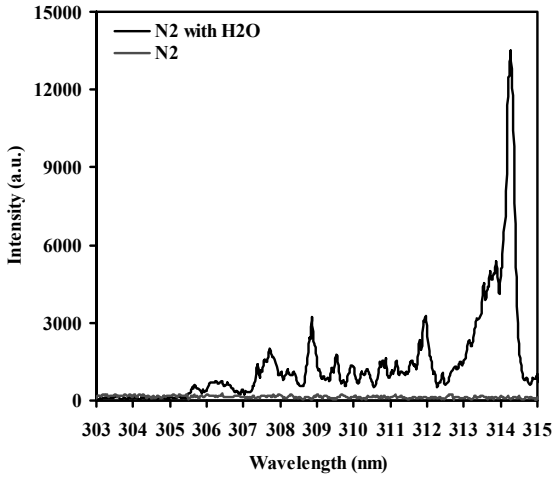

Fig. 12 Emission spectrum of microplasma generated by positive pulse in N_2 gas and in N_2 gas with water droplets for positive pulses.

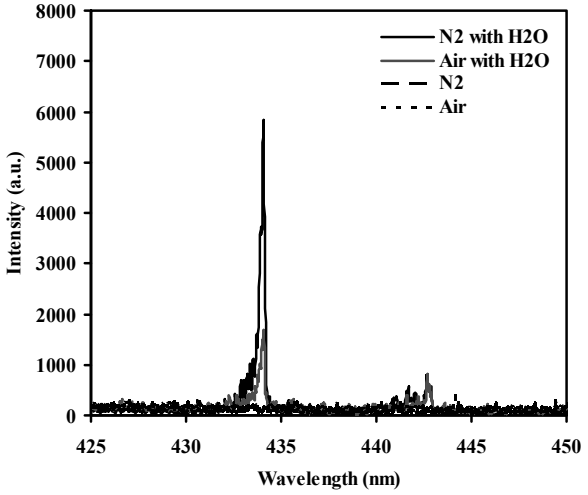

Fig. 13 Emission spectrum of microplasma discharge in N_2 gas or in air with water droplets, and without water droplets for positive pulses.

electron impact dissociation of water, according with reaction (3), did not occur without water droplets. Thus OH peaks were not observed.

H are generated by microplasma discharge in N_2 gas and air with water droplets according to relation (3). Emission spectrum of hydrogen Balmer line H-γ is shown at 434.1 nm (Fig. 13), using the interference optical filter with characteristics described for the emission spectrum presented in Fig. 10. It shows the peak of H-γ at 434.1 nm only for N_2 gas with water droplets and air with water droplets.

The data showed in Figs. 8 and 12 were measured with the same sensitivity of ICCD camera (micro channel plate (MCP) and phosphor screen) and also emission spectrum presented in Figs. 10 and 13 respectively. The peak intensities for the OH wavelengths and H-γ band system are lower for positive pulses.

That could be explained by the lower value of peak discharge current for the positive pulse of 0.9 A (Fig. 4(b)), comparing with the peak value of discharge current for negative of −2 A (Fig. 4(a)) at the same discharge voltage. Rise time of negative discharge pulse voltage is about 3 times faster than that of positive discharge pulse voltage (about 67 ns for negative pulse, about 210 ns for positive pulse). Difference of rise time depends on the MOSFET used in each circuit. It could make the difference of discharge current peak, even at the same discharge voltage.

4.3 Estimation of vibrational temperature for microplasma

The spectral bands of the 0–0 transitions of the second positive system of N_2 (λ=337.1 nm) and the first negative system of N_2^+(λ=391.5 nm) could be used for calculating the reduced electric field strength *E/N*, where *E* is intensity of electric field and *N* the concentration of neutral particles, as a function of their intensities ratio I_B(λ=391.5 nm)/I_C(λ=337.1 nm).

The reduced electric field strength in air with water droplets has the value around 500 Td (I_B/I_C = 0.12) (1 Td = 1×10^{-17} Vcm^2) for negative pulses (Fig. 6) and around 310 Td (I_B/I_C = 0.04) for positive pulses (Fig. 11) according with Ref. 18).

The vibrational temperature Tvib was evaluated using the N_2 second positive system ($C^3\Pi$ - $B^3\Pi$ band). We used the ratio 0-2 and 1-3 bands (λ = 380.5 and 375.5 nm) to calculate the temperature according to the following formula:

$$\ln (I_{0\text{-}2}A_{1\text{-}3}/I_{1\text{-}3}A_{0\text{-}2}) = E_{1\text{-}3}\text{-}E_{0\text{-}2}/Tvib \quad (12)$$

where $I_{0\text{-}2}$, $I_{1\text{-}3}$, $A_{0\text{-}2}$, $A_{1\text{-}3}$, $E_{0\text{-}2}$ and $E_{1\text{-}3}$ are the intensities, the transition probabilities, and the energy levels for the 0−2 and 1−3 bands respectively. The parameters for the calculation were obtained from reference.[19] According to equation (12) we have obtained for the emission spectra of the microplasma discharge in N_2 gas with water droplets using a positive pulse power supply (Fig. 11) a value of vibrational temperature Tvib = 1,450 K.

5. Conclusions

Diagnostics of microplasma are carried out by using a Marx generator, an ICCD camera and a photomultiplier. Estimation of vibrational temperature was also carried out to investigate the characteristics of microplasma. The experiments and calculation data conclude shown bellow:

1) Analysis of emission spectrum shows N_2 SPS, N_2 FNS, OH 3064 – Å system and H-γ band system for the microplasma discharge in N_2 gas with water droplets.

2) Emission spectrum of air with water droplets show N_2 SPS, N_2 FNS, and H-γ band system with lower intensities comparing with emission spectrum of microplasma discharge in N_2 with water droplets due to the quenching effect of oxygen atom and ozone.

3) Lifetime of emission signal measured by a photomultiplier tube corresponding to wavelength 337.1 nm of N_2 SPS was about 40 ns.

4) Emission spectrum intensities of microplasma generated with positive pulses are lower than the emission spectrum intensities generated with negative pulses. That could be explained by the lower discharge current generated at positive pulses at the same discharge voltage.

5) The calculated value of vibrational temperature of microplasma was Tvib = 1,450 K.

The factors which contributes to the inactivation processes of bacteria by using microplasma are known to be high intensity electric fields, radicals and UV light. Emission spectroscopy method proved the existence of OH, H radicals and UV light and could be helpful to understand the processes of bacteria inactivation.

References

1) K. Shimizu and T. Oda: Sci. Technol. Adv. Material., **2** (2001) 577
2) J. Machala, M. Janda, K. Hensel, I. Jedlovsky, L. Lestinska, V. Foltin, V. Martisovits, and M. Morvova: J. Mol. Spectrosc., **243** (2007) 194
3) F. Iza, G. J. Kim, S. M. Lee, J. K. Lee, J. M. Walsh, Y. T. Zhang, and M. G. Kong: Plasma Process. Polym., **5** (2008) 322
4) M. Tanino, W. Xilu, K. Takashima, S. Katsura and A. Mizuno: Int. J. Plasma Environ. Sci. Technol., **1** (2007) 102
5) K. Shimizu, M. Yamada, M. Kanamori and M. Blajan: IEEE Trans. Ind. Appl., **46** (2010) 641
6) T. Heeren, T. Ueno, D. Wang, T. Namihira, S. Katsuki and H. Akiyama: IEEE Trans. Plasma Sci., **33** (2005) 1205
7) J. L. Walsh and M. G. Kong: Appl. Phys. Lett., **91** (2007) 251504.
8) M. Blajan, M. Kanamori, H. Mimura and K. Shimizu: J. Inst. Electrostat. Jpn., **33** (2009) 8
9) M. Blajan, T. Ishii, M. Kanamori, H. Mimura, and K. Shimizu: *The 2009 Annual Meeting Record IEE Japan*, p.252 (2009)
10) R. Foest, M. Schmidt and K. Becker: Int. J. Mass Spectrom., **248** (2006) 87
11) E. Kamaratos: J. Quant. Spectrosc. Radiat. Transf., **110** (2009) 264
12) S. Zheng, L. Zhang, Y. Liu, W. Wang and X. Wang: Vacuum, **83** (2009) 238
13) K. V. Kozlov and H.-E. Wagner: Contrib. Plasma Phys., **47** (2007) 26
14) F. Liu, W. Wang, S. Wang, W. Zheng and Y. Wang: J. Electrostat., **65** (2007) 445
15) R. Ono and T. Oda: Int. J. Plasma Environ. Sci.Technol., **1** (2007) 123
16) N. Ezumi, D. Nishijima, H. Kojima, N. Ohno, S. Takamura, S. I. Krasheninnikov and A.Y. Pigarov: J. Nucl. Material., **266-269** (1999) 337
17) C.-H. Tsai, Y.-F. Wang, H.-H. Yang and C.-N. Liao: J. Hazard. Mater., **150** (2008) 401
18) K.V. Kozlov, H.-E. Wagner, R. Brandenburg and P. Michel: J. Phys. D: Appl. Phys., **34** (2001) 3164
19) W. Zyrnicki: Spectrosc. Lett., **25** (1992) 175